Turkish Journal of Remote Sensing and GIS
2020

Turkish Journal of Remote Sensing and GIS
Türk Uzaktan Algılama ve CBS Dergisi

Turk J Remote Sens GIS, March 2020, 1(1): 13-23
Journal homepage: http://www.dergipark.org.tr/en/pub/rsgis

Road Distress Measurements Using UAV
İHA Kullanarak Yol Bozukluk Ölçmeleri

Mustafa Zeybek[1]*, Serkan Biçici[2]

[1]*Artvin Coruh University, Engineering Faculty, Geomatics Engineering, 08100, Artvin/Turkey.*
[2]*Artvin Coruh University, Engineering Faculty, Civil Engineering, 08100, Artvin/Turkey.*

ORIGINAL PAPER

***Corresponding author:**
Mustafa Zeybek
mzeybek@artvin.edu.tr

doi:

Article history:
Received : 22.01.2020
Accepted : 16.03.2020
Published: 31.03.2020

Abstract

Maintenance and rehabilitation of the road are very serious actions. Therefore, road conditions should be inspected accurately before taking these actions. Manual and visual inspection in the field is the traditionally used method to monitor road conditions. However, it is time-consuming, labor-intense and costly. In addition, the traditional inspection method is unsafe directly for the inspectors and indirectly for primary users of the road, such as pedestrians and drivers. In this study, the unmanned aerial vehicle (UAV) was used to inspect the road condition. UAV technology is becoming a valuable tool for collecting data efficiently and accurately. The proposed method involved three steps. First, several images were acquired from a UAV flight. Then, these images were used to generate a three-dimensional (3D) point cloud, digital surface model and orthomosaic. Finally, road distresses were detected and measured from two-dimensional (2D) and 3D data. The measurements obtained from the proposed methodology were compared against the measurements obtained from the traditional inspection method. It was found that both measurements produced similar results. In conclusion, the use of the UAV measurement technique was found to be suitable for detecting road distress. Given the advantages of the proposed methodology, it can also be inferred that UAVs can be used instead of the traditional inspection method.

Keywords: *UAV, DSM, Orthomosaic, Road distress, Rut, Pothole*

Özet

Yolun bakımı ve iyileştirilmesi çok önemli eylemlerdir. Bu nedenle, bu eylemler yapılmadan önce yol koşulları doğru bir şekilde incelenmelidir. Arazideki manuel ve görsel olarak yapılan inceleme, yol durumunu izlemek için geleneksel olarak kullanılan yöntemdir. Ancak, bu, zaman alıcı, yoğun emek isteyen ve maliyetli bir yöntemdir. Buna ek olarak, geleneksel inceleme yöntemi sadece denetleyiciler için değil aynı zamanda yayalar ve sürücüler gibi yolun birincil kullanıcıları için de güvenlik problemi oluşturur. Bu çalışmada, yol durumunun incelenmesi için insansız hava aracı (İHA) kullanılmaktadır. İHA teknolojisi, verileri verimli ve doğru bir şekilde toplamak için önemli bir araç haline gelmektedir. Önerilen yöntem üç adımdan oluşur. İlk olarak, İHA uçuşundan birçok görüntü elde edilir. Daha sonra, görüntüler, üç boyutlu (3B) nokta bulutu, sayısal yüzey modeli ve ortomozaik oluşturmak için kullanılır. Son olarak, iki boyutlu (2B) ve 3B verilerden yol bozuklukları tespit edilir ve ölçülür. Önerilen metodolojiden elde edilen ölçüler, geleneksel inceleme yönteminden alınan ölçülerle karşılaştırılmıştır. Her iki ölçümden de nispeten benzer sonuçlar elde edilmiştir. Sonuç olarak, İHA ölçüm tekniğinin kullanımı yol bozukluklarını tespit etmek için uygundur. Önerilen yöntemin avantajları göz önüne alındığında, geleneksel inceleme yöntemi yerine İHA'nın kullanılabileceği sonucuna varmak oldukça güvenilirdir.

Anahtar kelimeler: *İHA, SYM,Ortomozaik, Yol bozuklukları, Tekerlek izi, Çukur*

1. Introduction

Imaging and analysis studies with unmanned aircraft vehicle (UAV) are carried out by different disciplines such as agricultural applications, urban mapping, topographic mapping, mining, coastal management, forestry and many other disciplines (Buğday, 2018; Doshi et al., 2015; Feng et al., 2015; Gulci, 2019; Johansen et al., 2019; Ochoa and Guo, 2019; Pijl et al., 2019; Tomastik et al., 2019). Besides, current practices and regulations for civil engineering are summarized by Yıldızel and Calış (2019). Thus, UAV systems become a valuable supporting tool for researchers and practitioners who deal with problems in many fields in fast decision-making, maintenance, and improvement of the applications. One of the areas that lately starts to use UAV technology is transportation engineering. Maintenance and rehabilitation of the road are very serious activities and the compressive data collections regarding the condition of the road are necessary to decide whether or not these actions are needed.

Traditionally, an assigned person goes out there and monitor the condition of the road. However, the traditional inspection methods are time-consuming, labor-intense and unsafe not only for drivers but also for other users of the road (Kim and Ryu, 2014; Saad and Tahar, 2019; Tan and Li, 2019). Today, some major software and application developers promote some civilian mobile applications. Users of the road provide information about road conditions, thanks to these mobile applications (Saad and Tahar, 2019). However, this information is limited and does not provide detailed information regarding road conditions. Over the years, new technologies and approaches are also introduced to inspect road conditions more effectively (Kim and Ryu, 2014).

Road inspection methods can be classified into three methods, namely, vibration-based method, two-dimensional (2D) image-based method and three-dimensional (3D) model-based method. In the vibration-based method, vibration due to road roughness is analysed in real-time. However, complete detail of the road is not inspected and the equipment for this method is costly (Eriksson et al., 2008). In the 2D image-based method, several images are processed by traditional image processing algorithms to inspect road conditions. Similarly, several technologies such as laser scanner, Kinect sensor and stereo vision are used to produce a 3D model of the road surface to inspect road conditions (Gezero and Antunes, 2019; Neupane and Gharaibeh, 2019). However, these methods are very expensive and require a long post-processing time (Kim and Ryu, 2014; Yadav and Singh, 2018).

UAV technology is also introduced to monitor road conditions. Several studies produce 3D models of road surfaces using UAVs. Zhang (2008) proposed a strategy for monitoring unpaved road conditions and developed a UAV based remote sensing system for obtaining road image and collecting road condition parameters. Inzerillo et al. (2018) proposed a semi-automated technique for diagnosing the road pavement distress with the use of structure from motion (SfM). Saad and Tahar (2019) and Tan and Li (2019) also developed a 3D model of the road surface from UAV images and then they used a software to detect road distress in the paved road. The authors stated that the proposed approaches are convienent to inspect road conditions.

In this study, we focus on the detection of road distress namely, rut and pothole on the paved road surface from point clouds, digital surface model (DSM) and orthomosaic obtained by UAV images. The main objective and contribution of this study are to inspect road condition using 3D model produced from low-cost UAV systems. The advantage of this approach over traditional inspection methods is that it is performed in normal traffic flow.

The remainder of the study is organized as follows. First, the study area is presented. Then, the proposed methodology is summarized. The results are discussed in the next section. Finally, the conclusion and final remarks are summarized in the last section.

2. Study Area

The study area is located in Artvin, Turkey. Figure 1 presents the study area and the location of the selected road. The local road that connects Artvin Coruh University Seyitler Campus and several areas such as the biggest high school in Artvin, a large-extent housing area and main Police Station etc. was selected. The inspected road, which was approximately 100 meters long, included several potholes and ruts.

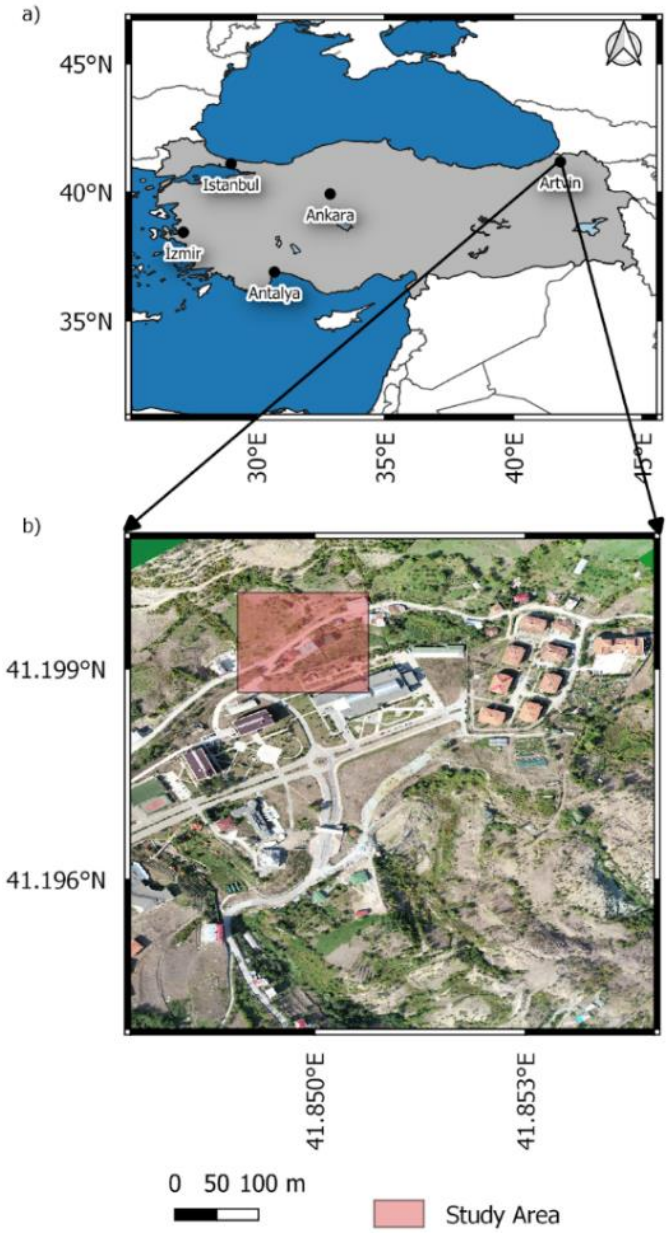

Figure 1. a) Location of the study area and b) selected road presented on the orthomosaic

3. Material and Methods

This study comprised four basi steps. The first step is to make traditional measurements in the field to which the proposed UAV-based method was compared. The next three steps are related to the proposed methodology in this study. Firstly, a UAV flight was conducted over the study area to capture the complete detail of the study area. Then, the images obtained from the flight were processed through an image processing software to generate photogrammetric products. The image processing step involved image alignment (initial processing), dense point cloud generation (point cloud and mesh), DSM and orthomosaic production (DSM- DTM and orthomosaic), as seen in Figure 2. In the last step, several road distresses were detected and measured from orthomosaic and DSM data using Global Mapper Software.

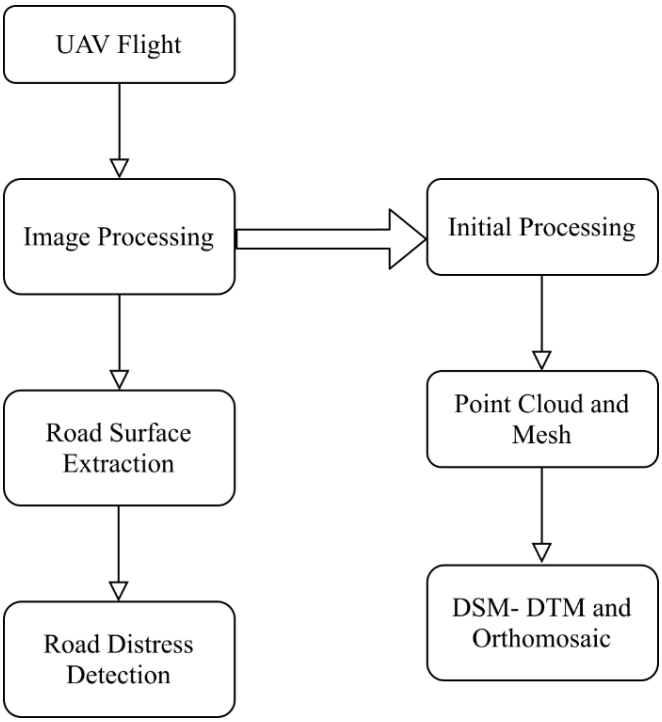

Figure 2. The overall methodology and image processing flowchart

3.1. UAV Device and Data Acquisition

DJI Phantom 4 RTK (P4RTK) mini UAV was used to investigate the selected road in this study. It is a low weight platform of 1391 g and has a flight time of about 25-30 minutes. It uses GPS, GLONASS, BeiDou and Galileo positioning systems. The camera of UAV has a 20 M CMOS sensor that offers 5472 × 3648 image resolution (Peppa et al., 2019). Ground sampling distance (GSD) is calculated as H/36.5 cm per pixel, where H denotes flying altitudes in the meter unit. The average flight altitude was around 5.5 m. It was important to capture images close to the ground to produce high-resolution data. Extra attention was paid not to fly close to the wires, buildings and vehicles in the flight area.

The production of photogrammetric data from UAVs is a preferred technology today. Thus, a wide range of software has been developed for flight planning, monitoring and communication between the operator and the UAV. Furthermore, automatic flight software do not require human control except for security reasons. Operation plans are prepared by selecting the region whose map will be produced. Then, the overlap and flight heights are set in parallel to the demand for high-resolution data.

In order to improve the image alignment accuracy and to acquire a detailed point cloud, in addition to the nadir (vertical) image, oblique image capturing can be performed. Figure 3 summarizes image acquisition types, which can be done with the UAV. The nadir direction image means that the direction of the lens is perpendicular to the ground or object. In this study, the oblique images were captured by adjusting the camera angle to 60^{o} degrees. Therefore, several images that give great detail condition of the road were obtained.

Since Fixed ground control point (GCP) marking method requires intense labor, it is not preferred in this study. Instead of indirect georeferencing of the reconstructed model, direct georeferencing methods is preferred. To do that, the images must always be geotagged with the GNSS/INS (Global navigational satellite systems and inertial measurement unit) data for the camera location and orientation of each image.

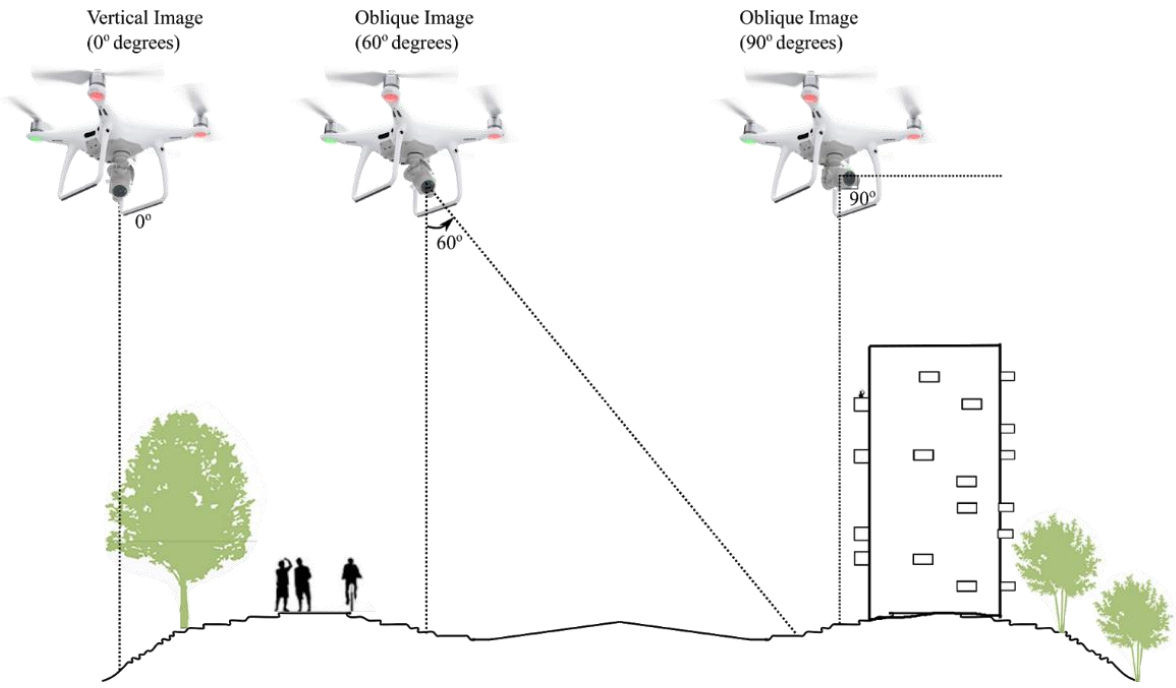

Figure 3. Image acquisition types: vertical and oblique images

3.2. UAV Data Process

For 3D modeling, different software packages that follow the standard structure from motion (SfM) workflow of oblique images and nadir direction images have been used in many studies Javernick et al. 2014). Some of the widespread SfM software packages are the Agisoft Metashape, Pix4DMapper, 3Df Zephyr, SURE, MicMac (MM), VisualSFM (VSFM), and ContextCapture. There are differences in the agorithims used in these softwares, specifically in image processing and matching step as well as some parameter setting. However, most of the software produce similar results in the alignment of the images, the production of dense point clouds, and the generation of a triangulated network in DEM and orthomosaic. In general, the only input data required by these software to perform 3D model generation are acquired images. If GCPs or GNSS/IMU data are available, this data contributes to the positioning of the generated maps.

In the study, the Pix4DMapper (www.pix4d.com) software was used to process acquired UAV images. In the first part of the 3D reconstruction process, the software prepares the images to match extracted features for bundle block adjustment using variations of the Scale Invariant Feature Transformation (SIFT) algorithm (Lowe, 2004).

Subsequently, the image locations and orientations are determined in the bundle block adjustment by evaluating the detected and matched key points after the image alignment process. Multi-view stereo (MVS) algorithms are used to produce detailed object surface geometries in high-dense 3D point cloud and triangular mesh models. Different algorithms are implemented in different software and these software do not provide detailed information on this step since they are commercial software. However, the semi-global matching (SGM) based stereo method is commonly used to achieve accurate, pixel-based matching with high stability. With the Pix4DMapper software, more than 20 million points were reconstructed in the dense point cloud production step.

Since the orthomosaic is a 2D map, the orthomosaic generation is different from photo stitching. Each pixel on this map contains the location and RGB color information. The orthomosaic has a uniform scale. Thus, 2D measurements, such as distance and area on the orthomosaics are possible. It does not contain camera distortion and therefore, it corrects the different scales based on the distance. The orthomosaic production is based on the orthorectification process, which uses undistorted images and DSM data.

3.3. Detection and Measurement of Road Distress

It is possible to measure the surface distress from any computer-aided design (CAD) or geographical information system (GIS) based software. In this study, the Global Mapper software was used to detect several ruts and potholes. Then, the features of ruts and potholes on the road surface were measured on a 3D DSM and 2D orthomosaics.

Four different features, namely, diameter, perimeter, length and depth were measured using the Global Mapper Software. Specifically, diameter, perimeter and depth were used for four potholes while length and depth were used for ruts. Firstly, a polygon was drawn manually on the 3D model and 2D orthomosaic for the detection of the pothole as shown in Figure 4. Then, the perimeter of the pothole was calculated as the sum of the length of each line that encloses the polygon. The diameter of the pothole was also measured as the maximum distance from one corner to another. In addition, the length of the rut was measured as the maximum distance with road distress.The depth of the potholes and ruts were calculated from the DSM profiles as shown in Figure 5 and Figure 6, respectively. In these figures, yellow lines represent the direction of profile. Road slope should be taken into account when taking the direction of profile. For this, it is possible to benefit from the contour lines. Thus, the profile following the contour line is taken and the slope factor is eliminated. Rut and pothole depths on the profile were obtained more accurately.

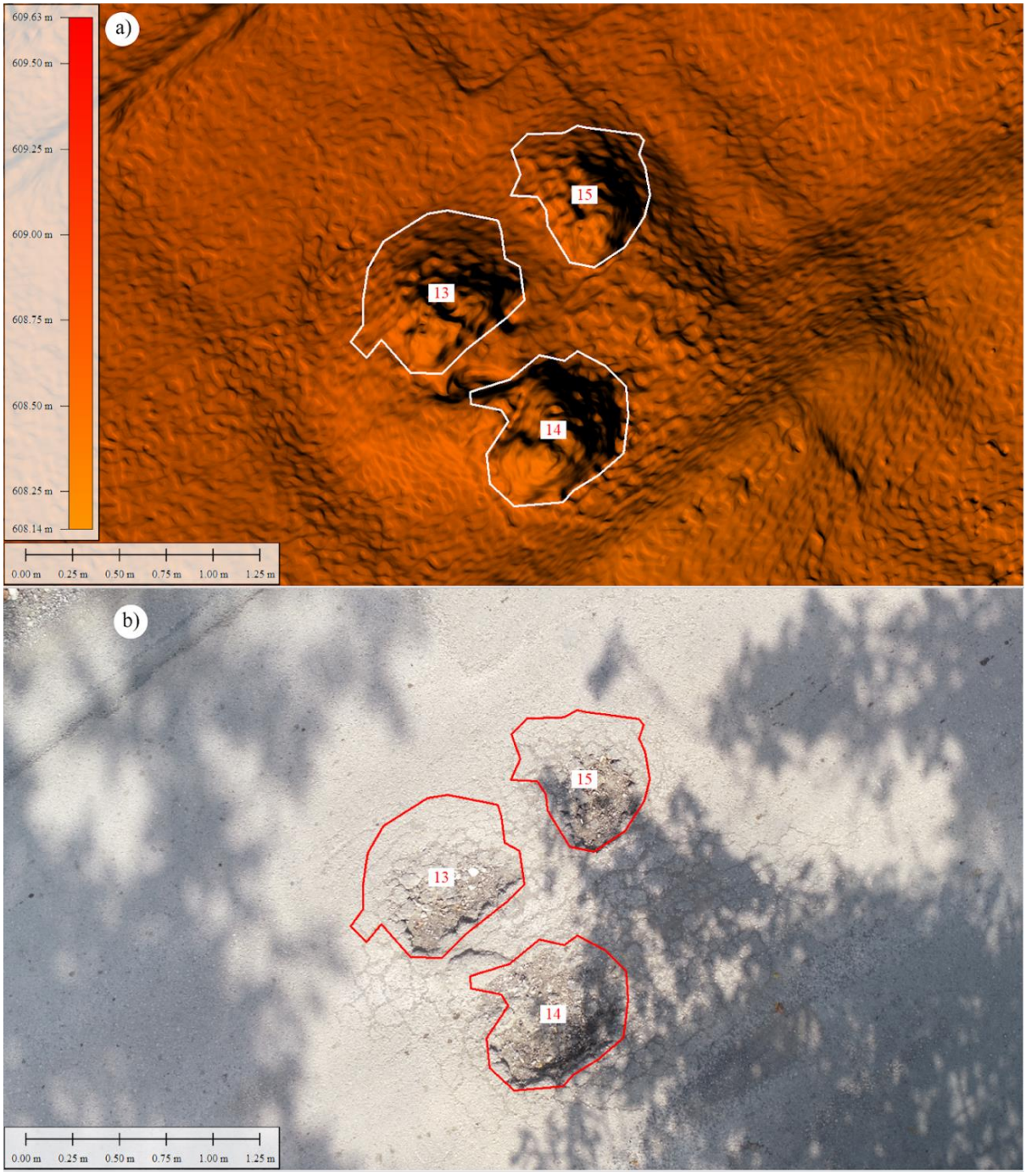

Figure 4. a) DSM and b) orthomosaic based pothole measurements

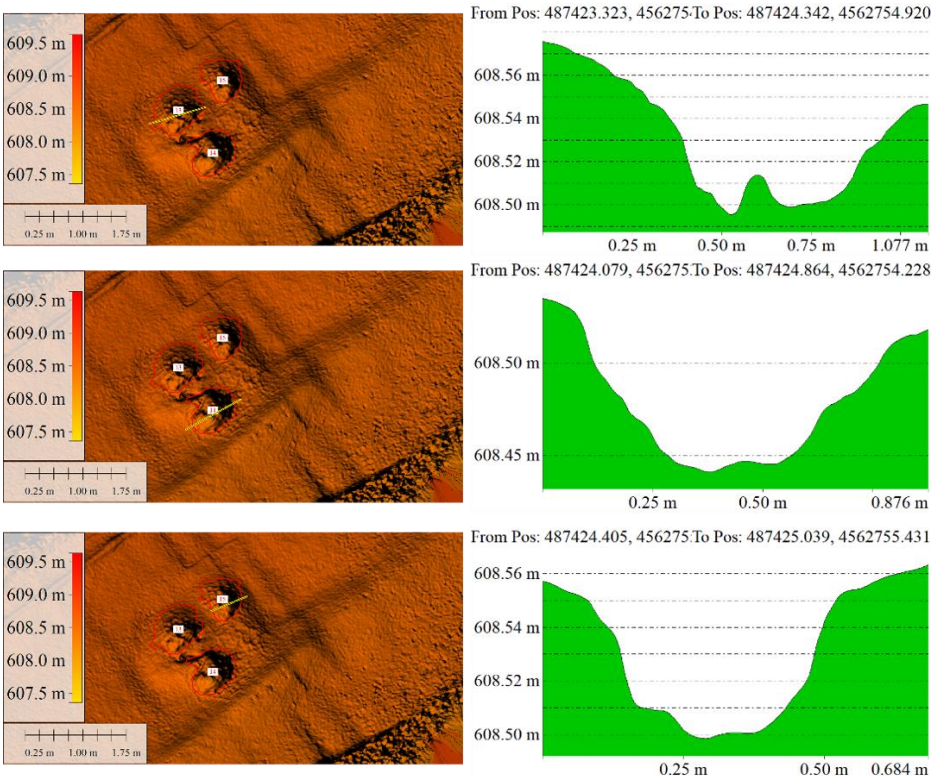

Figure 5. Pothole detection and measurement

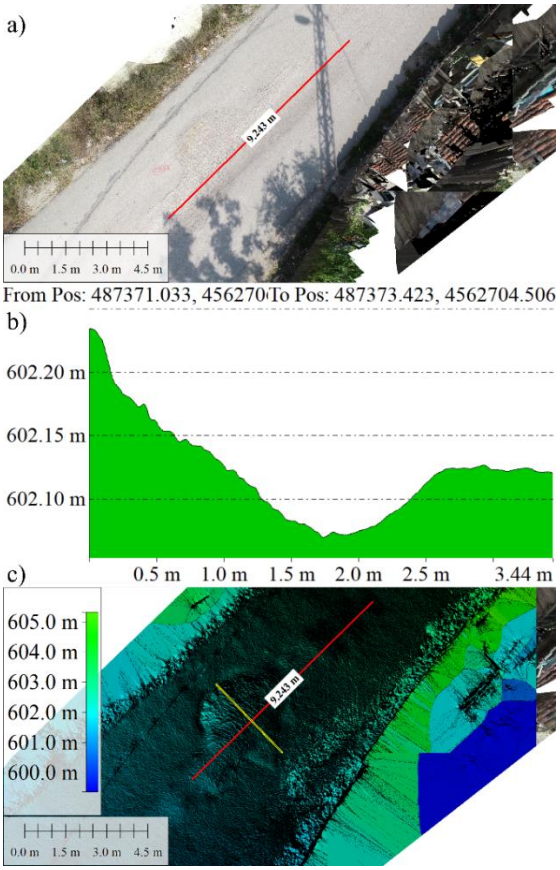

Figure 6. a) Rut length, b) profile perpendicular to the slope of the road and c) depth measurement on profile

4. Results and Discussions

Four potholes and seven ruts were detected in the study area. Four measures, namely diameter, length, perimeter and depth were measured manually in the field using a ruler and tape meter. The measures obtained from both field and Global Mapper Software are presented in Table 1. In addition, the accuracy assessment was conducted to compare the measurements obtained from the field and Global Mapper Software. Equation 1 shows the error (E) between two types of measurements.

$$E = M_{Software} - M_{Field} \quad (1)$$

where $M_{Software}$ is a measurement obtained using the Global Mapper Software and M_{Field} is a measurement obtained from field inspection. A positive error value means that the measurements obtained from the Global Mapper Software are greater than the measurements from field inspection while a negative error value means that the measurements obtained from the Global Mapper Software are lower than the measurements from field inspection. Zero error value is obtained when two types of measurements are equal to each other.

Table 1. Differences between measurements from field inspection and from the Global Mapper Software for diameter, length, perimeter and depth of the road distress.

Road Distress ID	Road Distress Type	Diameter (m)				Length (m)			
		Field	UAV	Error (m)	Error (%)	Field	UAV	Error (m)	Error (%)
Distress 1	Rut	-	-	-	-	9.200	8.895	-0.305	-0.033
Distress 2	Pothole	4.420	4.411	-0.009	-0.002	-	-	-	-
Distress 3	Rut	-	-	-	-	1.800	1.748	-0.052	-0.029
Distress 4	Rut	-	-	-	-	4.400	4.201	-0.199	-0.045
Distress 5	Rut	-	-	-	-	3.400	3.350	-0.050	-0.015
Distress 6	Pothole	1.030	1.015	-0.015	-0.015	-	-	-	-
Distress 7	Pothole	0.890	0.893	0.003	0.003	-	-	-	-
Distress 8	Pothole	0.760	0.761	0.001	0.001	-	-	-	-
Distress 9	Rut	-	-	-	-	6.500	6.345	-0.155	-0.024
Distress 10	Rut	-	-	-	-	1.900	1.946	0.046	0.024
Distress 11	Rut	-	-	-	-	9.900	9.564	-0.336	-0.034
Road Distress ID	Road Distress Type	Perimeter (m)				Depth (m)			
		Field	UAV	Error (m)	Error (%)	Field	UAV	Error (m)	Error (%)
Distress 1	Rut	-	-	-	-	0.092	0.093	0.001	0.011
Distress 2	Pothole	6.550	6.250	-0.300	-0.046	0.094	0.088	-0.006	-0.064
Distress 3	Rut	-	-	-	-	0.035	0.072	0.037	1.057
Distress 4	Rut	-	-	-	-	0.111	0.104	-0.007	-0.063
Distress 5	Rut	-	-	-	-	0.040	0.035	-0.005	-0.125
Distress 6	Pothole	3.280	2.958	-0.322	-0.098	0.077	0.074	-0.003	-0.039
Distress 7	Pothole	2.720	2.854	0.134	0.049	0.079	0.092	0.013	0.165
Distress 8	Pothole	2.250	2.514	0.264	0.117	0.069	0.065	-0.004	-0.058
Distress 9	Rut	-	-	-	-	0.091	0.092	0.001	0.011
Distress 10	Rut	-	-	-	-	0.030	0.044	0.014	0.467
Distress 11	Rut	-	-	-	-	0.060	0.072	0.012	0.200

When it comes to diameter, the error between two types of measurements ranges from 0.1 cm to 1.5 cm. These errors are considered small when taking into account the advantages of using the Global Mapper Software over field inspection. Similarly, a range from 0.1 cm to 3.7 cm was obtained when measuring the depth, which is also considered small. On the other hand, the errors are higher for length and perimeter. Specifically, a range from 2.0 cm to 15.5 cm was obtained for length and a range from 13.4 cm to 32.2 cm was obtained for the perimeter. It is most likely to have human-error in field inspection. For example, the shapes of the four potholes are irregular. It is hard to detect the boundary of these potholes in field, which leads to relatively higher human-error.

To assess the differences between two types of measurements, the root mean square error (RMSE) is also reported in Table 2. RMSE is defined as the following equation;

$$RMSE = \sqrt{\frac{\sum_{i=1}^{N}(M_{Software} - M_{Field})^2}{N-1}} \tag{2}$$

where N is the number of observation and $M_{Software}$ and M_{Field} are described as above.

Table 2. The root mean square error (RMSE) for diameter, length, perimeter and depth of the road distress

	Sample Size (N)	RMSE
Diameter	4	0.010
Length	7	0.076
Perimeter	4	0.301
Depth	11	0.009

These RMSE values were also consistent with the conclusions above. Smaller RMSE values were obtained when measuring the diameter, length and depth while larger RMSE values were obtained for the perimeter.

In addition to these discussions, a commonly used hypothesis test, so called *t*-test, was applied to statistically testing whether the mean of the differences between two types of measurements is equal to zero. The null hypothesis, H_0 and alternative hypothesis, H_A are as follows;

$$\begin{aligned} H_0 &: \mu_{error} = 0 \\ H_A &: \mu_{error} \neq 0 \end{aligned} \tag{3}$$

where μ_{error} is the mean of the differences between two types of measurements. The null hypothesis is rejected when the absolute value of the test statistic $|t_{test}|$ is greater than or equal to the critical t-value. The *t*-test results are shown in Table 3 for four different scenarios. For example, the four errors obtained when measuring diameters were used for the *t*-test. The test statistic $|t_{test}|$ is 1.1785 and the critical t-value is 2.7764 at 5% significance level. Since the test statistic is higher than the critical t-value, the null hypothesis is refused to reject. *t*-test is refused to reject for all scenarios. This means that both measurement types produce statistically similar results.

Table 3. The t-test results at 5% significance level

	$\|t_{test}\|$	Critical t values	Decision
Diameter	1.1785	2.7764	Refuse to reject null
Length	0.599	2.3646	Refuse to reject null
Perimeter	0.3525	2.7764	Refuse to reject null
Depth	1.2047	2.201	Refuse to reject null

The observations show that the measurements obtained using the Global Mapper Software are similar to those obtained from the traditional inspection method. In addition, the errors obtained in this study are similar to those obtained by Saad and Tahar (2019) and Tan and Li (2019). Given the advantages of using the Global Mapper Software over the traditional inspection method, it can be concluded that the Global Mapper Software produces reasonable measurements and they can be used instead of the traditional inspection method.

5. Conclusion

In transportation engineering, road condition inspection is a challenging process and requires a complete detailed picture of the road before taking maintenance or rehabilitation actions. However, traditional inspection methods are time-consuming, labor-intensive and unsafe for all users of the road.

UAV is a lately growing technology used in many fields, including transportation engineering. This study used the UAV data to detect road distress. Specifically, UAV was operated over the study area to evaluate the road condition through several images. Then, the Pix4DMapper software, a commercial image processing software, was used to produce the photogrammetric products. The image processing step involved image alignment, dense point cloud generation, DSM and orthomosaic production. Finally, several road distresses were detected and measured from the orthomosaic and DSM data using the GIS-based Global Mapper Software.

The measurements obtained from the Global Mapper Software were compared against the measurements from the traditional inspection method. It was found that both measurements produced relatively similar results.

We can conclude that the use of the UAV measurement technique is suitable for detecting potholes and ruts on the road surface. With the help of UAV images, detailed information about the road surface can be obtained from 2D and 3D data. In addition, it is easier to determine the ruts and potholes on the road surface in the office environment than to measure in the field because 3D model production is automatic, fast, safe and high resolution.

References

Buğday, E. (2018). Capabilities of using UAVs in forest road construction activities. *European Journal of Forest Engineering*, *4*(2), 56-62. doi:10.33904/ejfe.499784.

Desa, H., bin Azizan, M. A., Khadir, M. S. A., Suhaimi, M. S., Ramli, N. Z., & Hat, Z. (2019). Feasibility Study of UAV Implementation in Route Surveying. *Journal of Robotics, Networking and Artificial Life*, *6*(2), 84-88. doi:10.2991/jrnal.k.190828.003.

Doshi, A. A., Postula, A. J., Fletcher, A., & Singh, S. P. (2015). Development of micro-UAV with integrated motion planning for open-cut mining surveillance. *Microprocessors and Microsystems*, *39*(8), 829-835.

Eriksson, J., Girod, L., Hull, B., Newton, R., Madden, S., & Balakrishnan, H. (2008, June). The pothole patrol: using a mobile sensor network for road surface monitoring. In *Proceedings of the 6th international conference on Mobile systems, applications, and services* (pp. 29-39).

Feng, Q., Liu, J., & Gong, J. (2015). Urban flood mapping based on unmanned aerial vehicle remote sensing and random forest classifier—A case of Yuyao, China. *Water*, *7*(4), 1437-1455.

Fryskowska, A. (2019). Improvement of 3D Power Line Extraction from Multiple Low-Cost UAV Imagery Using Wavelet Analysis. *Sensors*, *19*(3), 700. doi:10.3390/s19030700.

Gezero, L., & Antunes, C. (2019). Road Rutting Measurement Using Mobile LiDAR Systems Point Cloud. *ISPRS International Journal of Geo-Information*, *8*(9), 404. doi:10.3390/ijgi8090404.

Gulci, S. (2019). The determination of some stand parameters using SfM-based spatial 3D point cloud in forestry studies: an analysis of data production in pure coniferous young forest stands. *Environmental monitoring and assessment*, *191*(8), 495. doi:10.1007/s10661-019-7628-4.

Inzerillo, L., Di Mino, G., & Roberts, R. (2018). Image-based 3D reconstruction using traditional and UAV datasets for analysis of road pavement distress. *Automation in Construction*, *96*, 457-469. doi:10.1016/j.autcon.2018.10.010.

Javernick, L., Brasington, J., & Caruso, B. (2014). Modeling the topography of shallow braided rivers using Structure-from-Motion photogrammetry. *Geomorphology*, *213*, 166-182. doi:10.1016/j.geomorph.2014.01.006.

Johansen, K., Erskine, P. D., & McCabe, M. F. (2019). Using Unmanned Aerial Vehicles to assess the rehabilitation performance of open cut coal mines. *Journal of cleaner production*, *209*, 819-833. doi:10.1016/j.jclepro.2018.10.287.

Kim, T., & Ryu, S. K. (2014). Review and analysis of pothole detection methods. *Journal of Emerging Trends in Computing and Information Sciences*, *5*(8), 603-608.

Lowe, D. G. (2004). Distinctive image features from scale-invariant keypoints. *International journal of computer vision*, *60*(2), 91-110. doi:10.1023/b:Visi.0000029664.99615.94.

Neupane, S. R., & Gharaibeh, N. G. (2019). A heuristics-based method for obtaining road surface type information from mobile lidar for use in network-level infrastructure management. *Measurement*, *131*, 664-670. doi:10.1016/j.measurement.2018.09.015.

Ochoa, K. S., & Guo, Z. (2019). A framework for the management of agricultural resources with automated aerial imagery detection. *Computers and Electronics in Agriculture*, *162*, 53-69. doi:10.1016/j.compag.2019.03.028

Peppa, M. V., Hall, J., Goodyear, J., & Mills, J. P. (2019). Photogrammetric assessment and comparison of DJI Phantom 4 pro and phantom 4 RTK small unmanned aircraft systems. *ISPRS Geospatial Week 2019*.

Pijl, A., Tosoni, M., Roder, G., Sofia, G., & Tarolli, P. (2019). Design of Terrace drainage networks using UAV-based high-resolution topographic data. *Water*, *11*(4), 814. doi:10.3390/w11040814

Saad, A. M., & Tahar, K. N. (2019). Identification of rut and pothole by using multirotor unmanned aerial vehicle (UAV). *Measurement*, *137*, 647-654. doi:10.1016/j.measurement.2019.01.093

Tan, Y., & Li, Y. (2019). UAV Photogrammetry-Based 3D Road Distress Detection. *ISPRS International Journal of Geo-Information*, *8*(9), 409. doi:10.3390/ijgi8090409.

Tomastik, J., Mokroš, M., Surový, P., Grznárová, A., & Merganič, J. (2019). UAV RTK/PPK Method—An Optimal Solution for Mapping Inaccessible Forested Areas?. *Remote sensing*, *11*(6), 721. doi:10.3390/rs11060721.

Yadav, M., & Singh, A. K. (2018). Rural road surface extraction using mobile LiDAR point cloud data. *Journal of the Indian Society of Remote Sensing*, *46*(4), 531-538. doi:10.1007/s12524-017-0732-4.

Yıldızel, S. A., & Calış, G. (2019). Unmanned Aerial Vehicles for Civil Engineering: Current Practises and Regulations. *Avrupa Bilim ve Teknoloji Dergisi*, (16), 925-932. doi:10.31590/ejosat.565499.

Zhang, C. (2008). An UAV-based photogrammetric mapping system for road condition assessment. *International Archives of the Photogrammetry. Remote Sensing Spatial Information Sciences. Sci*, *37*, 627-632.